DEUTSCHES ELEKTRONEN-SYNCHROTRON DESY

DESY SR 88-03
May 1988

A FAST LOW-NOISE LINE SCAN X-RAY DETECTOR

by

C.-C. Glüer, K. Engelke

II. Institut für Experimentalphysik, Universität Hamburg

W.-R. Dix, W. Graeff

Hamburger-Synchrotronstrahlungslabor HASYLAB at DESY, Hamburg

W. Kupper

Kardiologische Abteilung der II. Medizinischen Klinik, Universitäts-Krankenhaus Eppendorf, Hamburg

K.-H. Stellmaschek

Institut für Mathematik und Datenverarbeitung in der Medizin, Universitäts-Krankenhaus Eppendorf, Hamburg

ISSN 0723-7979

NOTKESTRASSE 85 · 2 HAMBURG 52

To be sure that your preprints are promptly included in the
HIGH ENERGY PHYSICS INDEX ,
send them to the following address (if possible by air mail) :

DESY
Bibliothek
Notkestrasse 85
2 Hamburg 52
Germany

DESY SR 88-03
May 1988

ISSN 0723-7979

A FAST LOW-NOISE LINE SCAN X-RAY DETECTOR

Claus-C. Glüer[1)#)]

Wolf-R. Dix[2)]

Klaus Engelke[1)]

Walter Graeff[2)]

Wolfram Kupper[3)]

Karl-H. Stellmaschek[4)]

[1)] II. Inst. f. Experimentalphysik, Universitat Hamburg

[2)] Hamburger Synchrotronstrahlungslabor HASYLAB at DESY, Hamburg

[3)] Kardiologische Abt. der II. Medizinischen Klinik, Universitäts-Krankenhaus Eppendorf, Hamburg

[4)] Inst. f. Mathematik u. Datenverarbeitung in der Medizin, Universitäts-Krankenhaus Eppendorf, Hamburg

[#)] present address: Department of Radiology, University of California, San Francisco, CA 94143

submitted to Med. Phys.

ABSTRACT

A fast low noise line scan detector (NIKOS) for digital radiography has been developed. It consists of an input x-ray phosphor screen that is coupled to a modified Reticon photodiode array by means of fiber optics with incorporated image intensifier. In its current version the detector can be operated with a maximum 600 Hz image acquisition rate for interlaced readout of two lines of 128 pixels each. Using a Gd_2O_2S:Tb x-ray input phosphor an afterglow of 25% in the first subsequent readout was observed. We also conducted afterglow measurements on several other powder and single crystal phosphors and the photodiode array. Using $CdWO_4$, the afterglow of the detector is limited by the lag of the photodiode array of 4.5%. By modifiying the readout electronics the noise of the photodiode array was reduced to below 1 greylevel, corresponding to a signal-to-noise ratio of 5200. The DQE* of the detector ranged from 0.18 to 0.4 for typical signal levels. The sensitivity was 10% saturation per 1.9mR entrance dose. The modular design of the NIKOS detector allows for individual selection of each component to optimize performance for a given application.

Keywords: digital radiography, digital subtraction angiography (DSA), radiation detectors, x-ray fluorescent screens, photodiode array.

* Detective Quantum Efficiency

I. INTRODUCTION

In modern digital radiography, detectors with large dynamic range are required. This is especially true for non-invasive procedures employing digital subtraction angiography (DSA), as the small subtracted signals are very sensitive to noise [1]. In addition, for fast moving objects like the heart the exposure time must be of the order of a few milliseconds. Using the recently developed method of DSA in energy subtraction mode [2,3,4] for the imaging of coronary arteries, the detector should offer a dynamic range of 1:10000 and an image or line acquisition rate of 1 kHz corresponding to an integration time of 1ms.

In clinical practise of cardiac imaging the most common x-ray detectors are x-ray image converter/TV-camera tubes. They typically consist of an electrostatically focussing intensifier tube with integrated x-ray phosphor input-screen (x-ray image converter) and a vidicon tube coupled either by lenses or by fiber-optics. These image converters are area detectors and their output signal allows for dynamic cine-mode imaging with 25 or 50 Hz. The performance of these detectors is adequate for most clinical applications. Recent reports, however, indicate that detectors based on solid state devices might offer the potential of significant improvement of image quality [1,5,6]. Some limitations of current image-converter/TV-camera tubes are:

- limited temporal resolution
- limited dynamic range
- large scatter-to-primary beam ratio.

For operation up to 60 Hz the modulation transfer function (MTF) can be as high as 0.9 [7]. For faster image acquisition rates, however, the MTF drops sharply. Most image converters are equipped with a P20 output phosphor screen that has an MTF (1kHz) of about 0.3 [7]. It may be even lower if the image converter is equipped with a slow TV camera.

The TV camera can also limit the dynamic range with values ranging from 1:120 [8] to 1:1500 [9], whereas image converters offer dynamic ranges in excess of $8*10^3$ [6].

When imaging smaller objects like blood vessels the image contrast is strongly reduced by the background of scattered radiation which for cardiac imaging can make up more than 90% of the detected signal [10]. This inherently limits the performance of any area detector. Scatter suppression devices like anti-scatter-grids may provide some improvement but they also partially absorb the primary radiation [11,12].

Factors such as low temporal resolution, small dynamic range and a large scatter-to-primary ratio limit image quality, particularly in cardiac imaging because of the fast moving coronary arteries and the vicinity of the lungs. Therefore, we developed a detector to be used with the NIKOS-system of non- invasive coronary angiography that employs synchrotron radiation as x-ray source ('NIKOS' - Nicht-invasive Koronarangiographie mit Synchrotronstrahlung). NIKOS is based on a dual energy (K-edge) DSA* approach for imaging of human coronary arteries with intravenous administration of the contrast material [13,14].

* DSA: Digital Subtraction Angiography

We report on the design of the NIKOS solid state detector which is part of that system but could also be used separately for other x-ray detection applications. Data are presented on its current performance and an outline of the upgrades that are currently under way is provided.

II. DETECTOR DESIGN

Due to the high scatter contribution to the image in area detectors we implemented a line scan system where the scattered radiation can be easily reduced to very low levels without diminishing the primary signal.

The modular detector system consists of five components:

- input x-ray phosphor screen,
- fiber optic 1,
- image intensifier,
- fiber optic 2,
- photodiode array including electronic readout.

Each could be modified individually to meet the requirements of different applications. The design of these components is described in the following sections.

For our application, we are attempting to achieve the following specifications:

- 1 lp/mm spatial resolution,
- 1 ms temporal resolution,
- a dynamic range of 1:10000,
- a suppression of scatter to the percent level,

- two parallel input lines with a width of 125mm, a height of 0.5mm and a spacing of 1.5mm.

Figure 1 shows a schematic of the overall design of the prototype detector (NIKOS I). The width of the input lines of NIKOS I is 63.5mm.

A. Input x-ray phosphor screen

In the phosphor screen the incident x-rays are converted to visible light. Phosphors are available as powders or as single crystals. Powders have to be settled on top of a substrate or an optical fiber by means of sedimentation techniques whereas single crystals can be coupled by optical resins. Criteria for selection of optimal phosphors for a given photon energy to be detected are:

- temporal resolution
- sensitivity
- absorption characteristics
- spatial resolution

The chemical composition of the phosphor mainly influences the first three properties, whereas the crystalline structure and the preparation technique have an impact on the last three items.

The current version of the detector (NIKOS I) uses a Gd_2O_2S:Tb phosphor powder that was settled on top of the fiber optics to a thickness of about 500μm, a size comparable to the desired spatial resolution. Gd_2O_2S:Tb was

chosen because it offers a relatively high sensitivity (13% [15]) and it can be handled easily (non-hygroscopic).

B. Fiber optic 1

The first fiber optic couples the phosphor screen(s) to the image intensifier. The information of each picture element (pixel) is guided separately in a randomly packed fiber bundle. There are two reasons for the use of this fiber optic configuration:

- matching a larger phosphor line to a given image intensifier input face,
- minimizing the crosstalk in the intensifier by spreading the pixels over the input face in an optimal manner.

If the latter aspect can be neglected and the input phosphor has a smaller size than the image intensifier the fiber optic can be omitted.

The numerical aperture of the glass fibers should be as large as possible to collect as many light photons as possible from the phosphor screen. Since the number of photons in front of the image intensifier strongly affects the noise of the final signal it is also important to minimize transmission losses and to pack the individual fibers of a bundle as tight as possible or to use one large single fiber.

The NIKOS I detector has two phosphor lines that are coupled to the image intensifier by means of 2 • 127 glass fiber bundles of 0.5 • 0.5 mm^2 cross section. Each bundle consists of 25 - 27 individual fibers (85µm diameter, numerical aperture 0.59). Whereas at the entrance face the 2 • 127

bundles are regularly packed side by side to form two parallel lines of 63.5mm length (Fig. 2a), at the image intensifier side they are evenly spread in a hexagonal structure over the image intensifier's input area of 25mm diameter (Fig. 2b). By means of this arrangement we obtain a center-to-center spacing between the bundles of about 1.3mm. At the exit each bundle has a diameter of about 0.7mm. The fiber length of approximately 13cm yields a smooth bending and negligible transmission losses (11% at λ=548nm, the wavelength of maximum emission of Gd_2O_2S:Tb).

The flexibility of the design is demonstrated by the possibility of easily feeding in two additional monitor signals which originate from a small phosphor screen in front of the patient to measure the incident x-ray flux. They are transmitted by two commercially available light guides that are plugged in the fiber optic 1.

C. Image Intensifier

The incorporation of an image intensifier is advantageous if the maximum incident signal intensity is not sufficient to saturate the photodiodes. The fiber geometry of the exit face of fiber optic 1 is identical to the fiber geometry of the entrance face of fiber optic 2. Therefore, it is essential to prevent distortion of the image in the intensifier. Other selection criteria are temporal and spatial resolution.

For NIKOS I, a proximity focussing image intensifier (Proxitronic Proxifier BV 2533 MX 35) with a fast X3 output phosphor (decay time 100ns) was chosen. This compact device (diameter 69mm, overall length 37mm for the

single stage version, 25 V DC power supply) can be arranged in a multi-stage setup. Whereas gains of about a factor of 10 W/W can be achieved routinely with a single stage and the fast X3 phosphor, 2 and 3 stage devices offer amplification of light intensity by factors of 100 W/W and 1000 W/W, respectively. Our 2-stage device showed a gain of 123 W/W. Background noise is low (equivalent background irradiation of 10^{-4}Lux). The limiting resolution is 17 lp/mm (at MTF=4%) for 2 stages. By having individual pixels spaced by 1.3mm, practically no inter-pixel cross-talk occurs. The input and output faces consist of fiber-optic faceplates with an individual fiber-diameter of 6μm. Hence, the image intensifier does not limit the spatial resolution of the detector.

D. Fiber optic 2

The second fiber optic couples the output face of the image intensifier to the photodiode array(s). At its exit face the geometrical arrangement of the fiber bundles and their cross section is adapted to the photodiode arrangement and size, respectively.

In the NIKOS I detector the individual fibers of each of the 256 fiber bundles are rearranged from a circular cross section of 0.7 mm diameter to a rectangular cross section of 100μm • 2.5mm. Precisely packed side by side, all fiber bundles result in an output cross section that exactly matches the input face of the photodiodes: 25.6mm • 2.5mm (Fig. 2c). Hence, by means of this special fiber optic geometry two lines of 63.5mm • 0.5mm of x-ray

phosphor plus two monitor fiber bundles are exactly coupled to a single photodiode chip.

E. Photodiode array and electronic readout

In the photodiode array the visible light is converted to an electrical charge and stored on the chip. The following readout electronics serially scan the photodiodes, amplify and digitize the signals. Hence, the detector collects integrated signals. By adjusting the gain of the image intensifier it can be adapted to a wide range of photon intensities.

The photodiode array of the NIKOS I detector is a single Reticon (EG & G Reticon, Sunnyvale, CA) RL 1024 SF integrated circuit (IC). It comprises 1024 photodiodes of 25μm • 2.5mm cross section, resulting in an active input area of 25.6mm • 2.5 mm. Hence, for our application, four photodiodes cover the area of one pixel. In order to minimize cross talk between adjacent pixels, the analog signal of 3 out of 4 photodiodes is integrated by a specially modified evaluation circuit. The 4th diode thus only serves as spacing element between pixels. The photodiodes are covered by a fiberoptic faceplate (6μm fibers), which facilitates coupling of fiber optic 2.

Reticon supplies a standard evaluation readout circuit (RC 1024 S), which, however, does not exploit the full potential of the photodiodes. In particular, the minimum sequential sampling period for the photodiodes is 0.2μs/photodiode, corresponding to 0.2ms/line of 1024 diodes (this will be called the integration time), whereas the RC 1024 S is limited to an integration time of 3.3ms. Hence, the photodiode IC is well suited for our

application but the evaluation circuit had to be modified. As of version NIKOS I the electronic modifications comprise:

- minimum integration time of 2ms,
- readout clocked by external trigger,
- separation of the photodiode IC and the preamplifiers from the main evaluation board thus achieving flexibility in its positioning.
- The modified electronic evaluation circuit yields an output signal up to 4.5V at saturation level. This signal is digitized by a 12 bit, 0.5 MHz ADC (type Datel 817) with a maximum input of 5 V. Hence the saturation level corresponds to 3650 greylevels.

III. DETECTOR PERFORMANCE

A. Temporal resolution

We tested the afterglow of the different phosphors and the temporal response of the Reticon in the millisecond-regime. The afterglow of the image intensifier (decay from 90% to 10% within 100ns) was not measured but taken from the data sheet because it is several orders of magnitude lower than that of the other components.

Figure 3 shows the principal setup for afterglow measurements on different phosphor screens. The probing x-ray beam (photon energy 33.17 keV, bandwidth appr. 150 eV) was collimated to about 0.2mm • 0.2mm and was chopped by a rotating disk of 100mm diameter. A small opening of 5mm cross-section allowed the beam to pass for a short period of 1ms with a repetition

rate of the disk's frequency of rotation of 27.3 Hz. The screen emitted visible light which was picked up by glass fibers, then guided to the photomultiplier tube (S-20), which was mounted outside the x-ray area in order to minimize background radiation.

The photomultiplier signal was fed into a multichannel analyzer (Canberra MCA 35plus), working in the multichannel-scaling-mode. At least 5000 sweeps, triggered by the position of the chopper disk were integrated in 1024 channels with 10μs time increment. The setup was adjusted by means of a $CdWO_4$ phosphor with very short afterglow (0.005% after 3ms [16]). The emitted light intensity was measured up to 6ms after the end of the x-ray pulse. Figure 4 shows the response of a $CdWO_4$ crystal, this pattern representing the closest approximation of a 1 ms rectangular response curve that was achievable with our experimental setup.

Figure 5 shows response curves of four commercially available phosphor powders along with results of two single crystal phosphors. The pulse height does not represent a measure of sensitivity since the number of collected x-ray pulses varied.

Afterglow intensity expressed as a percentage of the 1ms primary light signal level is presented in table I. Since a photodiode detector collects the signal over a period of (integration-)time (2ms for the NIKOS-I detector, 1ms for its final version) not only the afterglow after 1,2,3,4 ms is given but also the integrated signal S_I of the 1.,2.,3.,4. subsequent readout period of 1ms. Based on the formula

$$MTF(\nu) \simeq \frac{I_{max}(\nu) - I_{min}(\nu)}{I_{max}(\nu) + I_{min}(\nu)} \simeq \frac{100 - S_I}{100 + S_I}$$

the modulation transfer function (MTF) of an approximately rectangularly shaped pulse was estimated (usually the MTF is determined for periodic sinusoidal signals).

The results demonstrate that all of the three single crystal phosphors show afterglow of well below 0.1% after one millisecond, corresponding to a MTF(1kHz) ≃ 1. Of all the tested powder phosphors only (Zn,Cd)S:Ag,Ni with an MTF (1kHz) of 0.81 would be suited for our application. With the exception of ZnS:Ag all tested powder phosphors decayed approximately exponentially whereas ZnS:Ag showed a second time constant that resulted in multi-millisecond afterglow on the percent level.

Temporal response measurements of the Reticon to nanosecond LED light flashes yielded a mean lag of 4.5% in the first and a mean lag of 0.2% in the second subsequent readout after a signal of about 90% saturation had been applied to the photodiodes. The integration time was 2.7 ms.

B. Sensitivity

The sensitivity of the NIKOS I detector version was measured with a monochromatized beam at 33 keV, which was collimated down to a cross-sectional area of 0.25mm . The size was measured by exposing a high resolution x-ray film. The intensity of the monochromatic beam was determined by a NaI detector of known absorption characteristic. By careful

adjustment of lead shielding around the NaI detector the background radiation was reduced to below 2.5%.

For the following calculations we define the 'standard signal' to be 40000 counts per pixel (cpp). This standard signal was found to correspond to an average reading of 200 greylevels. Saturation of the detector occurs at 730 000 cpp of 33 keV photons, which is equivalent to $5 \cdot 10^{-6}$C/kg ionization dose.

C. Noise

Experimental results of noise measurements have only been obtained for the Reticon photodiode array. Noise figures for all other components are based on manufacturer's specifications and a theoretical model of noise statistics.

The noise characteristics of the phosphor screen have been modeled based on an extension of the theory of Hamaker [17]. This theory accounts for both x-ray absorption and light selfabsorption. For the x-ray energy range of 27 to 44 keV the predicted emitted light intensity has been shown to correspond well with experimental results (±10-20%, depending on phosphor material and screen weight [18,19]).

Based on optical properties such as numerical aperture and transmission losses and manufacturer's specifications the impact of the fiber optics and the image intensifier on the noise characteristics of the detector was found to be less than 6% [4].

For the Reticon, noise measurements were carried out with the modified evalution circuit. The photodiodes were illuminated by means of an LED which was positioned in such a way that the variation of illumination did not exceed the sensitivity variation of the individual diodes which is up to ±10%. A data set for a given illumination level contained 128 cycles with an integration time of 2ms. To avoid the above mentioned 'afterglow' effects several 'dummy' cycles preceeded the measurement.

For 9 different diodes mean and standard deviation of the data set were computed. By adjusting the current of the LED, the measurement was repeated at 8 different levels of light intensity, ranging from 5% to 90% saturation. The noise level given as the average standard deviation of the output of those 9 photodiodes is shown in Fig. 6.

The measurement was repeated after adding an electronic integrator to the evaluation circuit. This time the integrator signal, representing the total output of four adjacent photodiodes, was recorded for eight different photodiode-quadrupels. The statistical analysis was performed in the same way as for the individual photodiode measurement. For the single-diode-reading the noise level increases approximately linearly with the signal amplitude (from 1 greylevel at zero light amplitude to about 4 greylevels at saturation); it appears to be independent of light amplitude for the integrated signal (at less than 1 greylevel). The result is also shown in Fig. 6.

To discriminate noise originating in the Reticon photodiode chip from noise sources in the electronic evaluation circuit, the photodiode IC was replaced by a 'dummy photodiode IC' that allowed for generation of all

clocking pulses at constant zero preamplifier input signal level. This noise component was found to be 0.29 greylevels. This corresponds to the theoretical digitization error of $1/\sqrt{12}$ greylevels [20]. Hence, at low light levels, the modified evaluation circuit does not contribute measureably to the detector noise.

Using the results of fig. 6, we determined the signal/noise ratio (SNR) of the diode array and the modified evaluation board including the integrator. At saturation of 3650 greylevels a SNR of approx. 5200:1 at 2ms integration time was calculated. The standard signal of 200 greylevels would have an SNR of 284:1. Inclusion of all other noise sources of the detector reduces the SNR of the standard signal to about 120:1 [4], corresponding to a DQE of 0.35. Since noise does not increase linearly with signal flux the DQE increases with increasing flux. For a signal of 100000 cpp the DQE would be about 0.45 [4].

Since all data were calculated from the digitized data, they include a digitization error component of $1/\sqrt{12}$ greylevels.

IV. DISCUSSION

The design of the NIKOS detector was motivated by the demand for a fast low noise line scan detector. Our application is imaging of coronary arteries and for this purpose we are attempting to develop a detector with 1 lp/mm (0.5mm pixelsize) spatial resolution, a MTF (1kHz) of >0.9 and a SNR

of 200:1. This is necessary to achieve a SNR of 3:1 in the subtracted image assuming a 3% difference in the images to be subtracted. This 3% difference corresponds to the smallest vessel to be detected [21].

The spatial resolution of 0.5mm was achieved and found to be sufficient for the imaging of 1mm thick vessels. Because of radiation dose considerations this resolution should not be increased.

For the current version of our detector (NIKOS I) the temporal response has been shown to be limited by the Gd_2O_2S:Tb screen (MTF (0.5kHz) = 0.6) that had been chosen because of its relatively high sensitivity. For the Reticon and the image intensifier the corresponding MTF was determined to be 0.9 and 1, respectively. Results of afterglow measurements, however, showed that with single crystal x-ray phosphors such as $CdWO_4$, BGO and CaF_2:Eu an MTF of approx. 1 is achievable. Consequently, the upcoming version NIKOS II [22] will incorporate a $CdWO_4$ or CaF_2:Eu x-ray phosphor and an image intensifier of higher gain. With respect to afterglow, we expect the Reticon photodiode array to be the limiting component because of the observed lag in subsequent readouts. Since the signal of the 1024 photodiodes is read out sequentially, any influence of time constants of the readout electronics can be disregarded. We considered the reset signal insufficient to completely recharge the photodiodes during the available 250ns reset period. However, even a reduction of the time constant of the reset signal to 2ns (by incorporation of a QMOS buffer and a DMOS BSD 214 switch) left the lag of 4.5% unchanged.

For our application a lag of this magnitude may be tolerable. The readout frequency can be doubled by reading the even and odd photodiodes in parallel. By this we would achieve the required integration time of 1ms without increasing the lag.

In comparison to data of similar detectors, the achieved 2ms integration time of the NIKOS I detector compares favorably. The original Reticon readout device is limited to 3.3 ms. The MTF of current image converters that incorporate a P20 output phosphor is limited by its afterglow of 16% after 1ms to about 0.3. If not equipped with fast video cameras, the afterglow may last even longer, e.g. 50% after 100ms for the HIVICON tube, or 15% after 60ms for the SATICON tube [4].

For the complete NIKOS I detector, the DQE depends strongly on the flux of the input signal, with a range of 0.18 at 10000 cpp to 0.45 at 100000 cpp. A SNR of 200:1 is reached at 90000 cpp corresponding to a DQE = 0.44, whereas the standard signal of 40000 cpp has SNR = 120 with DQE = 0.35. The loss of DQE towards smaller input values is mainly due to the relatively low gain of the image intensifier, which amplifies the 40000 cpp input signal to a photodiode voltage of only 5.6% saturation. Even this sensitivity of 10% saturation level per 1.9mR entrance dose represents an 8-fold improvement over previous reports [23]. By enhancing the image intensifier gain (or reducing losses in the glass fibers) by a factor of 2 the 40000 cpp input signal would yield a 10% saturation output signal. For our application this would represent the optimum sensitivity (10% saturation per 1 mR) since it allows for a satisfactory DQE at standard signal levels and for detection of signals of up to 10-fold flux. For coronary imaging such a high flux can be

expected in areas where the blood vessels are partially overlayed by lung tissue.

Due to its lower sensitivity, incorporation of the $CdWO_4$ phosphor would require a higher image intensifier gain which could be achieved with a 3-stage version of the Proxifier. For this version, we expect a DQE (1kHz) of about 0.6 - 0.7 depending on the performance of the upgraded 1ms evaluation circuit.

V. SUMMARY

We have developed a fast low noise line scan detector that in its current version can be operated at up to 2ms integration time. Using a Gd_2O_2S:Tb x-ray input phosphor an afterglow of 25% in the first subsequent readout was observed. The DQE for typical signal levels ranged from 0.18 to 0.4. The sensitivity was 10% saturation per 1.9mR entrance dose. We are currently modifying the detector to a version of 12.5cm line width that incorporates a $CdWO_4$ phosphor screen, a 3-stage image intensifier and an upgraded evaluation circuit that promises performance specifications of MTF (1kHz) = 0.9-1.0, DQE (1kHz) = 0.6-0.7 and a sensitivity of 10% saturation at 1 mR entrance dose. The modular design of the NIKOS detector allows for individual selection of each component to optimize performance for a given application.

ACKNOWLEDGEMENTS

We gratefully acknowledge the support of the Werner Otto Stiftung.

REFERENCES

1. D. Sashin, E. J. Sternglass, B. S. Slasky, K. M. Bron, J. M. Herron, W. H. Kennedy, L. Shabason, J. Boyer, A. E. Pollitt, R. E. Latchaw, B. R. Girdany, R. W. Simpson, "Diode array digital radiography: initial clinical experience," AJR 139,1045 (1982).
2. E. Rubenstein, R. Hofstadter, H. D. Zeeman, A. C. Thompson, J. N. Otis, G. S. Brown, J. C. Giacomini, H. J. Gordon, R. S. Kernoff, D. C. Harrison, W. Thomlinson, "Transveneous coronary angiography in humans using synchrotron radiation", Proc Natl Acad Sci USA 83,9724 (1986).
3. W. R. Dix, K. Engelke, C. C. Glüer, W. Graeff, C. P. Höppner, K. H. Stellmaschek, T. Wroblewski, W. Bleifeld, K. H. Höhne, W. Kupper, "NIKOS - a system for non-invasive examination of coronary arteries by means of DSA with synchrotron radiation," Nucl Instr Meth A246,702 (1986).
4. C. C. Glüer, "Nicht-invasive Koronarangiographie mit Synchrotron- strahlung," (in german), PhD Dissertation, University of Hamburg, FR Germany (1986).
5. A. C. Thompson, F. S. Goulding, H. A. Sommer, J. T. Walton, E. B. Hughes, J. Rolle, H. D. Zeman, "A multi-element silicon detector for x-ray flux measurements," IEEE Trans Nucl Sci NS-29,793 (1982).
6. I. A. Cunningham, A. Fenster, "A photodiode array x-ray imaging system for digital angiography," Med Phys 11,303 (1984).
7. Data sheet 10/8/9860-720-02101, Philips, Eindhoven (1974).
8. U. W. Arndt, D. J. Gilmore, "X-ray television area detectors for macromolecular structural studies with synchrotron radiation sources," J Appl Cryst 12,1 (1979).

9. B. Arnold, H. Eisenberg, D. Borger, "Digital video angiography system evaluation," Appl Radiol 10,81 (1981).
10. L. T. Niklason, J. A. Sorenson, J. A. Nelson, "Scattered radiation in chest radiography," Med Phys 8,677 (1981).
11. R. A. Kruger, C. A. Mistretta, S. J. Riederer, "Physical and technical considerations of computerized fluoroscopy difference imaging," IEEE Trans Nucl Sci NS-28,205 (1981).
12. H. P. Chan, K. Doi: "Investigation of the performance of antiscatter grids: Monte Carlo simulation studies," Phys Med Biol 27,785 (1982).
13. W. R. Dix, K. Engelke, C. C. Glüer, W. Graeff, H. Jabs, K. H. Stellmaschek, W. Kupper, "NIKOS - A system for noninvasive examination of coronary arteries by means of digital subtraction angiography with synchrotron radiation, II. In-vivo investigations," DESY SR 86-10, Hamburg, FR Germany (1986), to be published in IEEE Comp Sci.
14. E. Rubenstein, G. S. Brown, J. C. Giacomini, H. J. Gordon, R. Hofstadter, R. S. Kernoff, J. N. Otis, W. Thomlinson, A. C. Thompson, H. D. Zeman, "Angiography by synchrotron radiation," Physica Scripta T19,487 (1987).
15. J. A. de Poorter, A. Bril: "Absolute x-ray efficiencies of some phosphors," J Elchem Soc 122,1086 (1975).
16. M. R. Farukhi, "Recent developments in scintillation detectors for x-ray CT and positron CT applications," IEEE Trans Nucl Sci NS-29,1237 (1982).
17. H. C. Hamaker, "Radiation and heat conduction in light-scattering material," Philips Res Rep 2,55 (1947).

18. G. W. Ludwig, "X ray efficiency of powder phosphors," J Elchem Soc 118,1152 (1971).

19. G. W. Ludwig, J. S. Prener, "Evaluation of Gd_2O_2S:Tb as a phosphor for the input screen of x-ray image intensifier," IEEE Trans Nucl Sci NS-19,3 (1972).

20. B. Widrow, "A study of rough amplitude quantization by means of Nyquist sampling theory," IRE T Circuit Theory 3,266 (1956).

21. W. Graeff, W. R. Dix, K. Engelke, C. C. Glüer, J. Heuer, W. Kupper, K. H. Stellmaschek, "NIKOS - a system for non-invasive coronary angiography with synchrotron radiation," in: H. U. Lemke, M. L. Rhodes, C. C. Jaffee, R. Felix (eds.), Computer Assisted Radiology, 278 (Springer-Verlag, Berlin 1987).

22. W. R. Dix, W. Graeff, J. Heuer, K. Engelke, C. C. Glüer, H. Jabs, Höppner CP, W. Kupper, P. Steiner, W. Bleifeld, K. H. Höhne, K. H. Stellmaschek, "Contributions of the NIKOS group to the 1st Frascati meeting on synchrotron radiation applications to digital subtraction angiography," DESY SR 87-07, Hamburg, FR Germany (1987), to be published in Conf Proc Ser of Societa Italiana di Fisica.

23. S. L. Fritz, L. T. Cook, "High resolution digital x-ray detector utilizing a discrete array of $CdWO_4$ scintillators and a self-scanned photodiode array," Med Phys 14,244 (1987).

TABLES

Table I: Afterglow of x-ray phosphors following 1ms irradiation

Phosphor	Signal [%] after 1ms	2ms	3ms	4ms	Integrated signal [%] betw. 0-1ms	1-2ms	2-3ms	3-4ms	MTF	MTF int.
$CdWO_4$	<0.1	-	-	-	<0.1	-	-	-	≈1	≈1
BGO	<0.1	-	-	-	<0.1	-	-	-	≈1	≈1
CaF_2:Eu	<0.1	-	-	-	<0.1	-	-	-	≈1	≈1
(Zn,Cd)S:AgNi	1.4	0.6	0.1	<0.1	10.8	1.1	0.5	<0.1	0.97	0.81
ZnS:Ag	8.9	4.5	3.0	2.4	25.2	5.7	3.4	2.4	0.84	0.60
Y_2O_2S:Eu	7.2	1.3	0.1	0.1	31.2	3.7	0.8	0.4	0.87	0.52
Gd_2O_2S:Tb	14.2	2.2	0.4	<0.1	44.2	7.2	1.2	0.1	0.75	0.39

FIGURE CAPTIONS

Fig.1: Schematic drawing of the NIKOS I detector version.

Fig.2: Arrangement of fiber bundles in the NIKOS I detector. Sectional views at

a) the input phosphor,

b) the in- and output faces of the image intensifier,

c) the photodiodes.

All dimensions given in millimeter.

Fig.3: Scheme of the experimental setup for measuring the temporal resolution of various phosphor materials.

Fig.4: Time spectrum of $CdWO_4$ luminescence emission after illumination with an x-ray pulse of 1 ms duration. Because of the very fast decay of $CdWO_4$ this spectrums closely reflects the shape of the input pulse.

Fig.5: Time response of various phosphors to a x-ray pulse as shown in Fig.4. (a)- (d) powders: a) Gd_2O_2S:Tb, b) Y_2O_2S:Eu, c) ZnS:Ag, d) (Zn,Cd)S:Ag,Ni; (e)-(f) single crystals: e) BGO, f) CaF_2:Eu.

Fig.6: Noise measurement at the output of the modified evaluation board of the Reticon IC with direct illumination of diodes by visible light

(upper curve) and after passing an analog integrator which integrates over 4 diodes (lower curve).

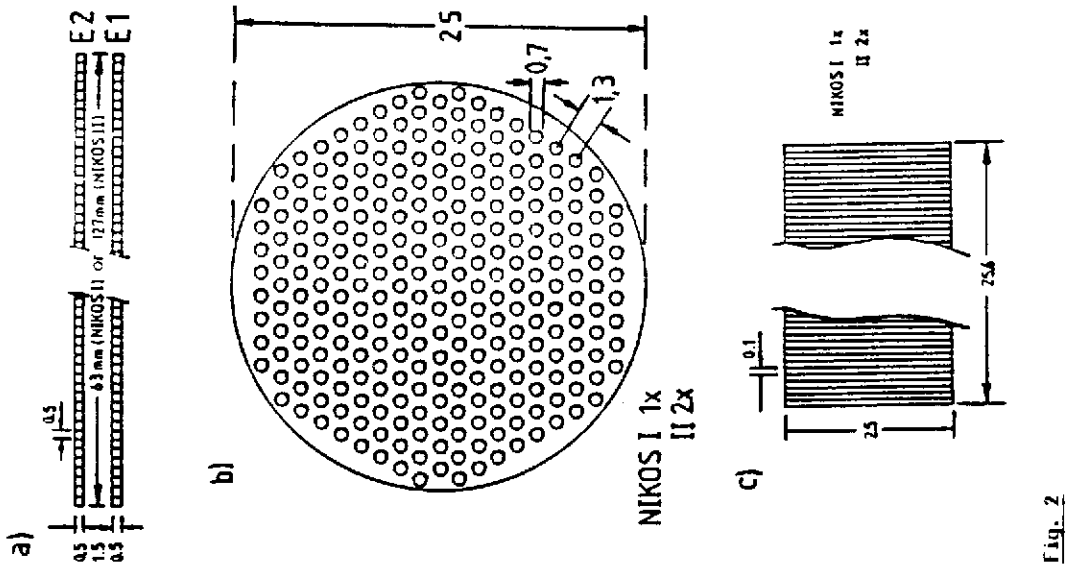
a)
E2
E1
0.5
63 mm (NIKOS II) or 127 mm (NIKOS III)
0.5
1.5
0.3
b)
25
0,7
1,3
NIKOS I 1x
II 2x
c)
NIKOS I 1x
II 2x
0.1
25
25.6

Fig. 2

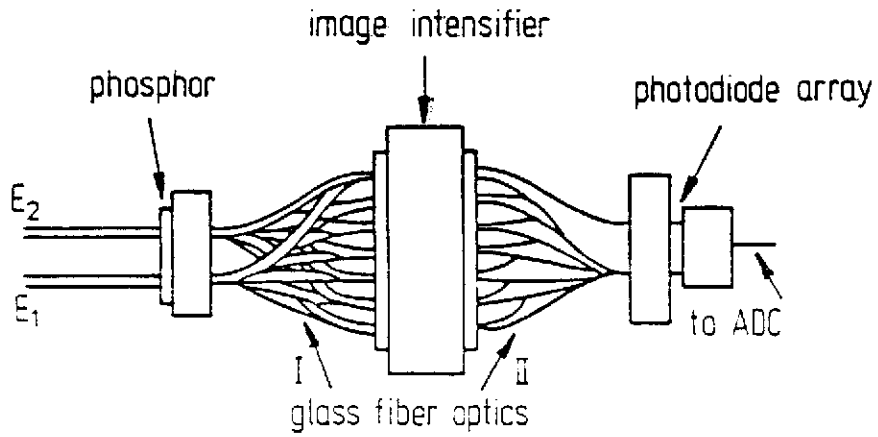
image intensifier
phosphor
photodiode array
E2
E1
to ADC
I
II
glass fiber optics

Fig. 1

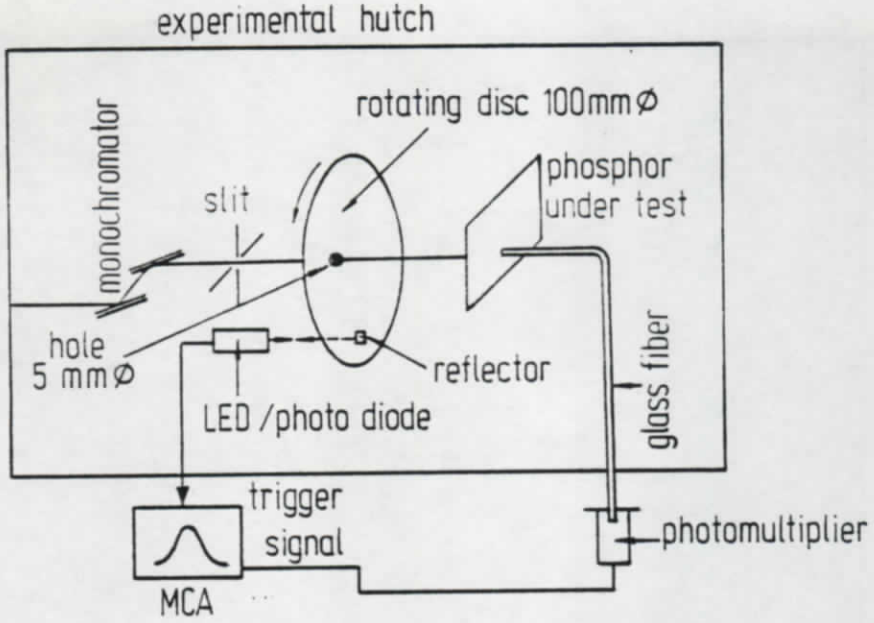
experimental hutch
monochromator
slit
rotating disc 100mmØ
phosphor
under test
hole
5 mmØ
reflector
LED /photo diode
glass fiber
trigger
signal
MCA
photomultiplier

Fig. 3

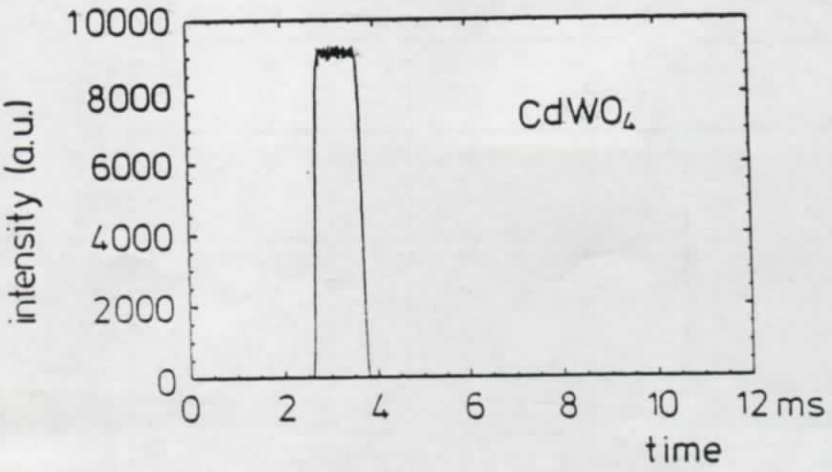
10000
8000
6000
4000
2000
0
intensity (a.u.)
CdWO4
0
2
4
6
8
10
12 ms
time

Fig. 4

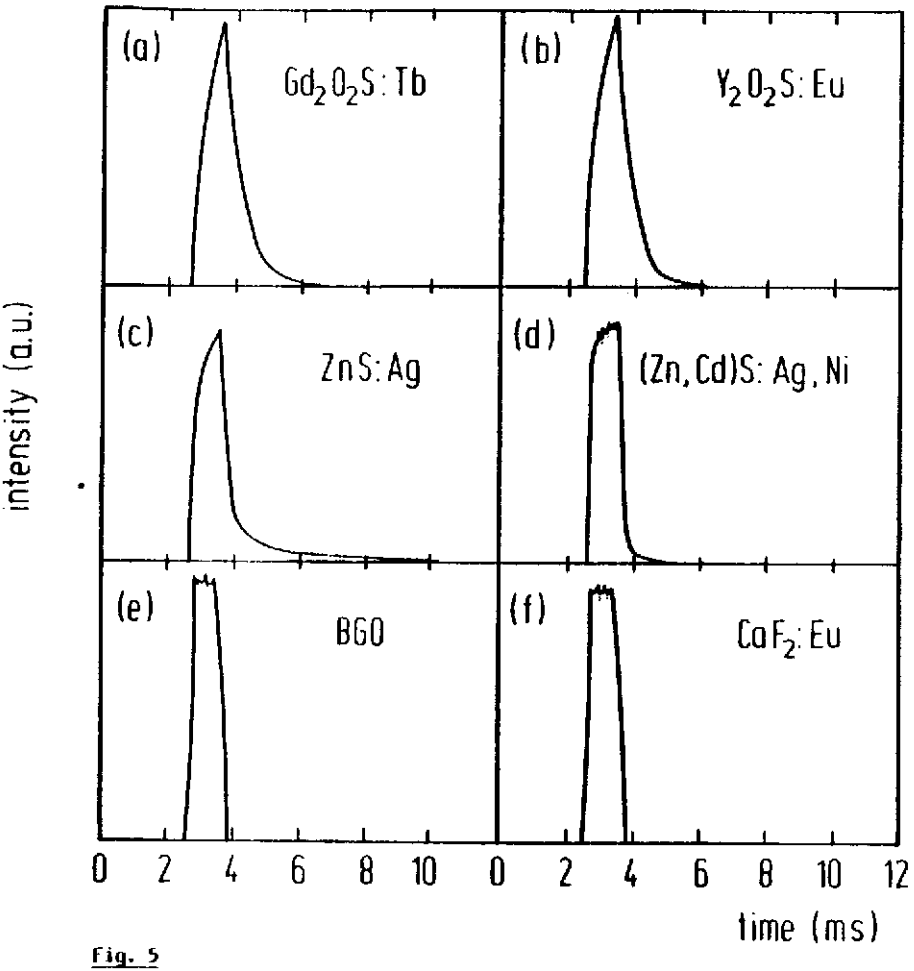
(a)
Gd_2O_2S: Tb
(b)
Y_2O_2S: Eu
(c)
ZnS: Ag
(d)
(Zn, Cd)S: Ag, Ni
(e)
BGO
(f)
CaF_2: Eu
intensity (a.u.)
0 2 4 6 8 10 0 2 4 6 8 10 12
time (ms)

Fig. 5

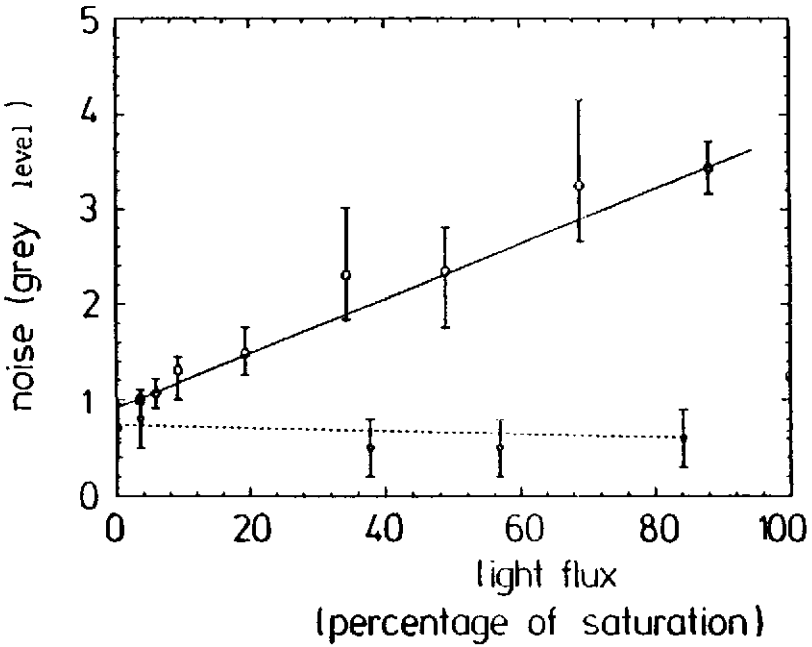
noise (grey level)
0 1 2 3 4 5
0 20 40 60 80 100
light flux
(percentage of saturation)

Fig. 6